Range calculations for IR rangefinder and designators

Walter R. Kaminski
United Technologies Research Center, Optics and Applied Technology Laboratory
Mail Stop D-63, P.O. Box 2691, West Palm Beach, Florida 33402

Abstract

Before a rangefinder or target designator design can be specified, the relationship between laser transmitter, receiver and range variables must be well understood. This paper presents results of calculations performed for that purpose using a rangefinder/designator systems model. Specifically, laser transmitter parameters such as wavelength (1.06, 3.8 and 10.6 micron), energy and pulsewidth and receiver parameters such as specific detectivity, field-of-view, signal-to-noise ratio and detector physical size were evaluated for numerous atmospheric conditions including rain and battlefield smoke. Target range was used as the primary basis of comparison. Major conclusions from the study were: (1) 10.6 micron wavelength is preferred for rangefinding and target designation when considering all weather, real battlefield operation, (2) for optimum performance, high pulse energy and short pulse width are desirable, (3) pulse energy per root pulse width of 100 to 1000 J-sec$^{-1/2}$ are recommended, (4) pulse energy per root pulse width varies logarithmically with range, thus pulse energy can be reduced substantially while producing only small variations in range, (5) performance improves when field-of-view and detector size decreases and signal-to-noise ratio and specific detectivity increases, and (6) the most sensitive receiver parameters were found to be detector size and field-of-view.

Introduction

Laser rangefinders and target designators have been used extensively by the military during the last 8 - 10 years. These laser devices operate in the visible to near infrared wavelengths (.63 micron to 1.06 micron). Their performance is acceptable under good weather conditions (high visibility) and tactically much has been learned. However, the enemy often strikes in bad weather and disperses smoke as a means of concealment. For these and other tactical reasons, laser systems operating from mid to far infrared wavelengths are becoming increasingly important. Palazzo and Wasilko[1] have analytically investigated laser target designation systems for wavelengths which meet the criteria of having a good atmospheric window, capable of being generated by a laser source having acceptable efficiency and being detectable and have concluded that future development should be based on the longer wavelengths (mid to far infrared).

Before proceeding, a distinction will be made between a rangefinder and a target designator. Figure 1 shows both configurations. A rangefinder consists of a laser transmitter which houses a pulsed laser, power supply, pulse forming electronics, coding electronics, a beam expander telescope and an optical sighting telescope. The receiver consists of focusing optics, optical bandpass filter, photodetector, signal amplification network, clock timer and range display. Range is determined from the time-of-flight measurement of a laser pulse to and from a target. In the target designator configuration, the same laser transmitter as described above is used to acquire a slow moving or stationary target. A seeker/tracker on an air launched rocket, cannon, or missile provides guidance to the target based upon signals reflected from the target.

Before a rangefinder or target designator design can be specified, the tradeoff between laser transmitter and receiver variables must be well understood. Although both rangefinders and target designators are considered in this paper, the majority of results are for the rangefinder configuration but general conclusions are found to apply to the designators as well.

Systems analysis

The maximum range for a rangefinder is determined by the following factors: average pulse energy, pulse duration, atmospheric attenuation, target reflectivity, optical beam divergence

and receiver sensitivity. The link model presented here is an extension of the one given by Palazzo and Wasilko[1] and modified as necessary by the author.

Link model

The link model considers only direct detection. Target interaction is treated in a simplified manner, and the beam angular uncertainty over the target area is assumed to be negligibly small. The analysis starts by considering a target designator where the laser transmitter is located remote from the receiver (see Figure 2). The parameters considered in this model are summarized in Table 1.

For a Lambertian reflector, the receiver intensity is given by

$$I_R = \frac{W_p \rho \cos\theta}{\pi (10^{10}) (R_T^2)} \exp [- \sigma (R_T + R_D)] \quad (1)$$

where the factor of 10^{10} converts I_R to units of J/cm^2. The term $(\rho \cos\theta/\pi)$ relates to a Lambertian surface, the term $(1/R_T^2)$ accounts for beam divergence and the term $\exp [- \sigma (R_T + R_D)]$ accounts for atmospheric attenuation. At maximum acquisition range the optical signal exceeds the equivalent noise signal by a prescribed signal-to-noise ratio, S/N, so that at maximum range I_R is also given by

$$I_R = \frac{1}{A_R \tau} (S/N) (NEP) (t_p) \quad (2)$$

Table 1. Link Model Parameters

R_T	=	Maximum acquisition range, km
R_D	=	Designation range, km
R	=	Range to target for a rangefinder, km
W_p	=	Pulse energy, J
t_p	=	Pulse duration (FWHM), sec
σ	=	Atmosphere attenuation coefficient, km^{-1}
I_R	=	Received optical intensity, J/cm^2
ρ	=	Effective target reflectivity
θ	=	Beam incidence angle, deg.
Δf	=	Receiver bandwidth, Hz
NEP	=	Noise equivalent power, W
NEI	=	Noise equivalent irradiance, W/cm^2
$NEI/\sqrt{\Delta f}$	=	K_2 = NEI per root cycle, $W/Hz^{1/2} - cm^2$
K_1	=	Minimum signal-to-noise ratio
$(K_3)^2$	=	Time-bandwidth product at receiver, sec-Hz
A_R	=	Receiver area, cm^2
τ	=	Transmission of receiver optics
η	=	Detector quantum efficiency
q	=	Electron charge 1.6022×10^{-19} C
c	=	Speed of light, 3×10^{10} cm/s
h	=	Planck's constant, 6.626×10^{-34} J-s
N_b	=	Background radiance, W/cm^2-sr-μ
$\Delta\lambda$	=	Bandpass of optical filter, μm
FOV	=	Field-of-view, sr
f/no	=	f-number of receiver optics
D*	=	Specific detectivity, $cm\text{-}Hz^{1/2}\text{-}W^{-1}$
A_D	=	Detector area, cm^2
i_{AMP}	=	Amplifier noise current, Amps
S	=	Detector responsivity, Amps/Watt

Since $NEI = NEP/A_R\tau$

$$I_R = (S/N) (NEI) (t_p) \quad (3)$$

NEI is proportional to $\sqrt{\Delta f}$ and S/N will be taken as a constant in the study ($K_1 = S/N$), we write

$$I_R = K_1 \underbrace{\left(\frac{NEI}{\sqrt{\Delta f}}\right)}_{K_2} \underbrace{\sqrt{\Delta f}\ \sqrt{tp}}_{K_3}\ \sqrt{tp} \tag{4}$$

In direct detection the square root of the time - bandwidth product is taken as a constant K_3 so that I_R can be expressed as

$$I_R = K_1\ K_2\ K_3\ t_p^{1/2} \tag{5}$$

where $(NEI/\sqrt{\Delta f}$ has been replaced by K_2 in order to simplify notation. Equating (1) and (6) gives the desired relationship connecting the maximum acquisition range, R_T, with the laser parameters, W_p, and t_p, thus establishing the optical link.

$$\frac{W_p}{\sqrt{t_p}} = C\ R_T^2\ \exp\left[\sigma\ (R_T + R_D)\right] \tag{6}$$

$$\text{where; } C = \frac{\pi\ K_1\ K_2\ K_3\ (10^{10})}{\rho\ \cos\theta} \tag{7}$$

For a rangefinder, $R_T = R_D = R$ in equation (6).

The atmospheric attenuation coefficient is actually composed of 4 contributions; a scattering and an absorptive coefficient associated with constituents in the atmosphere plus a scattering and an absorption coefficient due to the aerosol content.

$$\sigma = K_m + \sigma_m + K_a + \sigma_a + \sigma_{H2O} \tag{8}$$

The various terms are discussed later in this paper. If rain is present then an σ_{rain} term is added to (8) and K_a and σ_a are either zero or have some nominal value associated with the relative humidity. The σ_{H2O} term is an attenuation coefficient associated with the water vapor continuum. For the case of battlefield smoke which usually covers a local region, an attenuation coefficient, σ_{smoke}, multiplied by the beam path length through the smoke field, L, must be used to modify equation (6) as follows

$$\frac{W_p}{\sqrt{t_p}} = C\ R_T^2\ \exp\ 2\left[\sigma\ (R_T + R_D) + \sigma_{smoke}\ L\right] \tag{9}$$

Receiver parameters

Three sources of noise affect the receivers' response; (1) detector noise $(K_2)_{R,\ DET}$ which is characterized by the specific detectivity D*, (2) $(K_2)_{R,\ AMP}$ due to amplifier noise current, and (3) noise due to background irradiance $(K_2)_B$ from solar reflection and blackbody radiation.

The total noise contribution in terms of $NEI/\sqrt{\Delta f} = K_2$ is given by

$$K_2 = \left[(K_{2_{R,\ AMP}})^2 + (K_{2_{R,\ DET}})^2 + (K_{2_B})^2\right]^{1/2} \tag{10}$$

The noise equivalent background irradiance per-root-cycle, K_{2_B}, is obtained from the relationship

$$K_{2_B} = \left[(2\ hc)\ \left(\frac{1}{\eta}\right)\ \left(\frac{FOV}{A_R \tau}\right)\ \left(\frac{\Delta\lambda}{\lambda}\right)\right]^{1/2}\ (N_b \times 10^4)^{1/2} \tag{11}$$

where N_b is the background radiance. The amplifier noise current per-root-cycle when divided by the detector responsivity, S, and product $A_R\tau$ gives $K_{2_{R,\ AMP}}$

$$K_{2_{R,\ AMP}} = (i_{AMP}/\sqrt{\Delta f})/(S\ A_R \tau) \tag{12}$$

The detector responsivity is calculated from the relationship

$$S = q \frac{\eta\lambda}{hc} \tag{13}$$

The term $K_{2_{R,\ DET}}$ is calculated from equation (14)

$$K_{2_{R,\ DET}} = 2\left(\frac{f/no}{D^*\tau}\right)\left(\frac{FOV}{\pi A_R}\right)^{1/2} \tag{14}$$

The field-of-view, FOV, for the detector is given as a function of the total conical angle θ.

$$FOV = \pi \sin^2(\theta/2) \tag{15}$$

the f stop number, f/no, is given in terms of the conical angle, θ, detector size, W, and receiver optic diameter, D_R,

$$f/no = W/(\theta\ D_R) \tag{16}$$

Although this analysis uses simplifying assumptions, for example, the target interaction and simple beam propagation, it predicts the fundamental scaling relationship in simple form and appears to be consistent with trends of experimental data on CO_2 rangefinder performance. Data on a CO_2 rangefinder produced by Ferranti Ltd. of Edinburg, Scotland[2] was used to compare theory and experiment. For a CO_2 pulsed TEA laser with W_p = .015 J, t_p = 50 nsec, calculations predicted a maximum range of 4.9 km. Actual measurements gave a range of 5.3 km. The variation between the predicted and measured is most likely due to assumed values of N_b and $K_{2_{R,\ AMP}}$.

Range calculations

The link model discussed in the previous section was utilized in a study to determine the tradeoffs between the various laser transmitter and receiver parameters with target range as the primary basis of comparison. The following parameters have been investigated to date and are discussed in this section.

Laser transmitter:

(1) Wavelength (λ = 1.06, 3.8 and 10.6 micron)*
(2) Laser Energy Per Pulse, W_p
(3) Laser Pulse Width, t_p

Receiver:

(1) Specific Detectivity, D*
(2) Voltage Signal to Noise Ratio, S/N
(3) Field of View
(4) Detector Physical Size, W

Atmosphere:

(1) 5 Atmospheric Models
  . Sub Arctic Winter (SAW)
  . Mid Latitude Winter (MLW)
  . Sub Arctic Summer (SAS)
  . Mid Latitude Summer (MLS)
  . Tropical (TRP)
(2) 4 Levels of Visibility (Aerosol Model)
(3) Rain

* Although primary interest is in the 3.8 - 10.6 micron wavelength, 1.06 micron is carried in the analysis because it represents a state-of-the-art system and offers a basis for comparison.

TABLE 1

ATMOSPHERIC ATTENUATION COEFFICIENTS

K — ABSORPTION σ — SCATTERING M — MOLECULAR a — AEROSOLS

	ATMOSPHERIC MODELS										VISIBLE RANGE, km							
	SAW		MLW		SAS		MLS		TRP		1		3		5		23.5	
λ,μ	K_m	σ_m	K_m	σ_m	K_m	σ_m	K_m	σ_m	K_m	σ_m	K_a	σ_a	K_a	σ_a	K_a	σ_a	K_a	σ_a
1.06	$< 10^{-6}$	9.39×10^{-4}	$< 10^{-6}$	8.91×10^{-4}	$< 10^{-6}$	8.38×10^{-4}	$< 10^{-6}$	8.20×10^{-4}	$< 10^{-6}$	8.04×10^{-4}	0.48	1.66	0.160	0.550	9.63×10^{-2}	3.31×10^{-1}	1.98×10^{-2}	6.79×10^{-2}
	NO WATER VAPOR CONTINUUM																	
3.8																		
$P_3(7)$	6.13×10^{-2}	$< 10^{-6}$	5.60×10^{-2}	$< 10^{-6}$	5.16×10^{-2}	$< 10^{-6}$	5.10×10^{-2}	$< 10^{-6}$	5.07×10^{-2}	$< 10^{-6}$	0.35	0.35	0.120	0.113	0.07	0.07	0.07	0.014
$P_2(8)$	0.29×10^{-2}	↓	0.35×10^{-2}	↓	0.3×10^{-2}	↓	0.73×10^{-2}	↓	0.95×10^{-2}	↓	↓	↓	↓	↓	↓	↓	↓	↓
$P_2(7)$	0.67×10^{-2}	↓	1.34×10^{-2}	↓	2.83×10^{-2}	↓	4.09×10^{-2}	↓	5.35×10^{-2}	↓	↓	↓	↓	↓	↓	↓	↓	↓
$P_2(6)$	0.611×10^{-2}	↓	1.39×10^{-2}	↓	3.11×10^{-2}	↓	4.57×10^{-2}	↓	6.00×10^{-2}	↓	↓	↓	↓	↓	↓	↓	↓	↓
H_iO	0.165×10^{-2}	↓	0.48×10^{-2}	↓	1.25×10^{-2}	↓	1.92×10^{-2}	↓	2.72×10^{-2}	↓	↓	↓	↓	↓	↓	↓	↓	↓
											H_2O CONTINUUM							
10.6	4.12×10^{-2}	$< 10^{-6}$	7.94×10^{-2}	$< 10^{-6}$	2.01×10^{-1}	$< 10^{-6}$	3.58×10^{-1}	$< 10^{-6}$	5.79×10^{-1}	$< 10^{-6}$	0.120	0.102	4.6×10^{-2}	3.9×10^{-2}	2.67×10^{-2}	2.27×10^{-2}	5.48×10^{-3}	4.65×10^{-3}
	WATER VAPOR CONTINUUM INCLUDED IN K_m VALUES																	

$$\alpha_E = K_m + \sigma_m + K_a + \sigma_a + \alpha H_2O$$

$$\tau_{dB} = 4.34\alpha_E$$

SAW — SUB ARCTIC WINTER
MLW — MID LATITUDE WINTER
SAS — SUB ARCTIC SUMMER
MLS — MID LATITUDE SUMMER
TRP — TROPICAL

Battlefield environment:

(1) 4 Types of Tactical Smoke

Evaluation of atmospheric, background and target parameters

This section deals with the numerical evaluation of atmospheric, background and target parameters.[3]

Atmospheric attenuation

For coherent laser sources, the atmospheric attenuation is due to absorption and scattering by molecules on specific lasing lines, water vapor continuum and aerosols. The relative importance of these various attenuation phenomena are strongly wavelength-dependent. For example, at 1.06 micron aerosol scattering is the predominant loss mechanism and the absolute humidity has a negligible effect. Thus, as the aerosol concentration increases or visibility decreases, the 1.06 micron transmission is severely limited. However, at 10.6 micron the aerosol scattering and absorption are very small relative to the absorption due to the water vapor continuum and CO_2 molecules. Thus, the 10.6 micron system is not sensitive to visibility, but it is strongly sensitive to the absolute humidity.

In recent years, much work has been done to evaluate the atmospheric propagation characteristics at the high resolution representative of narrow-band laser lines.[4] This work has been used for the specific wavelengths of interest to define the comparative atmospheric attenuation characteristics over a wide range of operational environments used in this study. The five standard atmospheric models represent a spectrum from the cold low absolute humidity environments, Sub Arctic Winter (SAW) model, to hot high absolute humidity environment, Tropic Model (TRP). Each of these models were combined with an Aerosol Model representative of clear day (23.5 km visible range, V_R) to hazy day (5 km, V_R). This model was also extrapolated to visible ranges of 1, 3 and 5 km. Thus, four visible range conditions are considered for each of the five standard atmospheres. Table 2 contains the detailed attenuation coefficients used in this study.

The Nd:YAG (1.06 micron) and CO_2 (10.6 micron) lasers operate on a single line. The DF laser, on the other hand, operates in a multiline mode with its power divided over about 32 discrete lines. For this case, the attenuation characteristics are evaluated by numerical averaging the absorption and scattering coefficients of the four lines which produce about 50 percent of the energy output. The four DF laser lines used are $P_3(7)$, $P_2(6)$, $P_2(7)$, and $P_2(8)$.

Background radiance

Table 3 gives values for background radiance for both terrain background and sky background operation for 1.06, 3.8 and 10.6 micron wavelengths. The data were extracted from work performed by Fradin[3]. Additional information is also available from the Handbook of Military Infrared Technology[6] and the RCA Electro-Optics Handbook.[7]

Table 3
Comparison of Terrain and Background Radiance

WAVELENGTH (μ)	TERRAIN BACKGROUND		SKY BACKGROUND	
	CONDITION	RADIANCE, N_b ($w-cm^{-2}-sr^{-1}-\mu^{-1}$)	CONDITION	RADIANCE, N_b ($w-cm^{-2}-sr^{-1}-\mu^{-1}$)
1.06	HI – SUNNY DAY		HI – CLEAR SKY	1×10^{-3}
	GRASS, CONCRETE	1×10^{-3}	OVERCAST SKY	0.8×10^{-3}
	SNOW	1×10^{-2}	SUNLIT CLOUD	1×10^{-2}
	LO – DARK NIGHT	$<1 \times 10^{-8}$	LO – DARK NIGHT	$<10^{-8}$
3.8	HI – CONCRETE	2×10^{-5}	HI – CLOUD	5×10^{-5}
	LO – WINTER GRASS	2×10^{-6}	LO – DAYTIME SKY	5×10^{-6}
10.6	HI – SUNLIT GROUND	1×10^{-3}	HI – CLEAR SKY	0.8×10^{-3}
	SUNLIT SAND	1.25×10^{-3}	(HORIZON)	
	LO – NIGHT TIME GROUND	0.7×10^{-3}	LO – ZENITH SKY	0.3×10^{-13}
	NIGHT TIME SAND	0.9×10^{-3}		

Target reflectivity

Target reflectivity as a function of wavelength depends in a complex manner on the transmission and absorption characteristics of the material or surface coatings. It also depends on the surface roughness and the correlation length of the roughness relative to the wavelength. Much data has been taken on various samples in terms of hemispherical reflection, defined as the ratio of the total energy over a hemisphere, to the incident energy on the sample surface. Data of this type are summarized in Figure 3 in terms of reflectivity versus wavelength.[3] The data were obtained over a broadband, and the mid-bandwidth points are plotted. The data are representative of the battlefield environment. Fradin[3] recommends that a target reflectivity value of 0.1 be used and assumed to be independent of wavelength for first order analysis.

Atmospheric conditions

Figures 4(a) through 4(i) show the variation of the laser correlating parameter ($W_p/\sqrt{\tau_p}$) as a function of target range (R) for 5 atmospheric models (SAW, MLW, SAS, MLS, TRP) and 3 levels of visibility (V_R = 1, 5, and 23.5 km). High terrain background conditions were assumed and held fixed for this analysis. This situation appears to be the most likely background condition encountered in battlefield use of a rangefinder and target designator. Figures 4(a) through 4(c) are for a 1.06 micron Nd:YAG laser source utilizing an uncooled Si detector. Table 4 lists the various detector and receiver optics parameters used in this study for the 1.06 micron wavelength calculations. The values used in Table 4 are representative of current rangefinder/designator systems. The parameters have been defined previously. Notice that rangefinder performance is independent of atmospheric conditions and only dependent upon visibility (aerosol content, fog) at 1.06 micron. More will be said later when comparing rangefinder performance as a function of wavelength.

Table 4. Parameter Values Used in Study

Parameter	Wavelength, Microns 1.06	3.8	10.6
Detector	Si (300°K)	Hg Cd Te (77°K)	Hg Cd Te (77°K)
η	.5	.5	.5
FOV (sr.)	.015	.015	.015
$\Delta\lambda$ (μm)	.0212	.076	.212
τ	.5	.5	.5
A_R (cm^2)	80.	80.	80.
i_{amp} (amps)	6.0×10^{-9}	6×10^{-9}	6.0×10^{-9}
Δf (Hz)	1×10^{7}	1×10^{7}	1×10^{7}
D* ($cm\text{-}Hz^{1/2}\text{-}w^{-1}$)	3×10^{11}	1×10^{11}	2×10^{10}
S/N	7.	7.	7.

Figures 4(d) through 4(f) are for a 3.8 micron DF chemical laser source utilizing a cooled (77°K) HgCdTe detector. The values of atmospheric absorption and scattering coefficients used were based upon averaging over 4 of the strongest DF lasing transitions as previously discussed. Table 4 lists the various detector and receiver optics parameters used in the study for 3.8 micron wavelength calculations. These figures indicate that rangefinder performance is effected by both atmospheric conditions and visibility and, furthermore, the spread in performance with atmospheric condition increases as visibility increases. This means that as the aerosol content increases, it becomes dominant over prevailing atmospheric conditions.

Figures 4(g) through 4(i) are for a 10.6 micron CO_2 laser source utilizing a cooled (77°K) HgCdTe detector. Table 4 lists the various detector and receiver optics parameters used in the study for 10.6 micron wavelength calculations. At 10.6 micron, performance is highly dependent upon atmospheric conditions but relatively independent of visibility. More will be said about this situation later.

At this point it would be well to summarize what has been learned from the link analysis which is plotted in Figures 4(a) through 4(i).

1. Rangefinder performance at 1.06 micron is very sensitive to the visual range or aerosol content essentially independent of the absolute humidity or precipitable water water vapor.

2. Performance at 10.6 micron is very sensitive to the absolute humidity and is least sensitive to visual range.

3. The 3.8 micron performance is moderately sensitive to visual range and less sensitive to absolute humidity.

4. The 3.8 micron performance is better than that of 10.6 micron except at high absolute humidity and low visual ranges.

5. The 3.8 micron performance is also better than that of 1.06 micron except at very high relative humidities and high visual ranges.

6. The link analysis shows that for optimum performance, high W_p and short t_p are desirable.

7. The most striking result is the manner which range, R, varies with the laser pulse parameters, W_p, and t_p. There is a logarithmic relationship between $W_p/\sqrt{t_p}$, and R. Thus $W_p/\sqrt{t_p}$ can be reduced substantially while producing only small variations in range. Since t_p is a square-root function, it contributes an even smaller change in range. These trade-offs will be very important in the light of weight and volume considerations.

A value of $W_p/\sqrt{t_p}$ = 1000 J-sec$^{1/2}$ was chosen to minimize the number of variables in the studies which follow. In retrospect this chosen value of $W_p/\sqrt{t_p}$ is probably on the high side, nevertheless, it is representative and subsequent results are intended to show trends only.

Figure 5 shows plots of target range versus visible range for 1.06, 3.8 and 10.6 microns for $W_p/\sqrt{t_p}$ = 1000 J-sec$^{-1/2}$. Two plots are presented; one is for the mid-latitude winter (MLW) atmospheric model and the other is for a mid-latitude summer (MLS) model. These models represent average world weather conditions. For the MLW model we can see that λ = 10.6 micron operation is favored up to a visible range of 2.6 km, thereafter the 3.8 micron wavelength is superior. The 10.6 micron wavelength performance is better than the 1.06 micron wavelength up to a visible range of 8.5 km. For the MLS atmospheric model, 3.8 micron performance is superior to 1.06 and 10.6 micron up to a visible range of 16 km, thereafter the 1.06 micron wavelength is better. 10.6 micron is better than 1.06 micron up to a visible range of 2.6 km.

Calculations similar to those presented previously for the rangefinder were also performed for the target designator. Figure 6 shows the laser pulse parameter as a function of range with weather model as a parameter for a 10.6 micron transmitter. High terrain background conditions and a 5 km visibility were assumed. The designation range, R_D, was 2 km and the beam incidence angle φ was taken as 45°. Figure 6 shows trends that are very similar to those already shown in Figure 4h for the rangefinder with similar comments applying. If designation range is varied, then the resulting performance is as shown in Figure 7. Figure 7 shows $W_p/\sqrt{t_p}$ as a function of range with R_D as a parameter for a 10.6 micron radiation source, high terrain background, MLW weather model and 5 km visibility condition. A value of $W_p/\sqrt{t_p}$ of 100 to 1000 is typically chosen.

Battlefield Smoke

Up to this point, all weather rangefinding favors operation at the mid to far infrared wavelengths with 3.8 micron being favored over 10.6 micron. However, when the real battlefield situation is encountered with copious amounts of dust, smoke and hydrocarbons present, the situation changes. Detection at 10.6 micron is found to be superior to 1.06 micron and better than 3.8 micron. The effects of operating electro-optic equipment in a battlefield smoke environment have been reported elsewhere[8,9,10] but will be summarized here.

Basically, smoke is an artificial environment of local extent and is usually nonuniform and of short duration. It is an evolving environment and cannot be characterized in precise

terms. However, studies to date show that smoke obscures targets by a combination of three effects: (1) attentuation of the irradiance received from the target and background, (2) degradation of image resolution by narrow angle forward scattering, and (3) superposition of glare over the target/background image. The relative importance of each of these effects depends upon the particle characteristics (size and complex index of refraction), wavelength (visible or infrared), and detector characteristics. Attenuation of light within a cloud is due jointly to scattering and absorption. In general, the amount of scattering is greatest when the particle size and the wavelength are approximately equal. At these wavelengths the total attentuation is nearly independent of the absorption coefficient. On the other hand, when the wavelength becomes large compared to the particle size, scattering is negligible and absorption dominates.

Experimental results show that tactical smoke provides very effective screening in the visible and near infrared (up to 1.5 micron) but is relatively transparent to far infrared (8-12 micron). Persistence of a smoke field varies from a few seconds to many minutes, depending on wind and other conditions. Measurements show that tactical smoke consists of particles having radii generally less than 1 micron.

Extinction coefficients for smoke agents are presented in Table 5 and based upon data reported by Holst et. al.[8] The smoke considered are red phosphorous, fog oil, hexacloroethane (HC) and acid fog (FS). The optical transmission of 2 of these 4 smokes is illustrated in Figure 8 as a function of path length and wavelength. These quantities are related by the expression

$$\tau_s = \exp(-\alpha CL) \tag{17}$$

where τ_s is the transmittance through the smoke cloud, α is the extinction coefficient, C is the smoke concentration (assumed to be 0.1 g/m^3 for this study) and L is the path length. Effective screening is a function of source contrast and detector sensitivity and, in general, occurs for a fractional transmittance of 10^{-1} to 10^{-2}. If we take $\tau_s = 5.0 \times 10^{-2}$ as a mean value and take a typical smoke field to be from 50 to 100 meters in extent, Figure 8 shows that a 1.06 micron wavelength rangefinder cannot detect the target. A 3.8 μm rangefinder cannot detect a target when fog oil is used but can when FS is used. The 10.6 micron rangefinder can detect a target for all smokes and path lengths. This is shown more graphically in Figure 9.

Table 5. Extinction Coefficient (m^2/gm)

	Visible	1.06 μm	3.39 μm	10.6 μm	3-5 μm	8-12 μm
Fog Oil	3.20	3.64	0.96	0.047	0.36	0.10
Red Phosphorous	3.36	1.93	0.34	0.47	0.29	0.27
FS	3.85	2.19	0.31	0.15	0.17	0.23
HC	2.38	N/A	0.35	0.79	0.20	0.53

This figure illustrates the reduction in range capability for the three wavelengths considered when both FS and fog oil obscure the target for a range of smoke path lengths.

Rain

The effect of rainfall on propagation of laser radiation was also investigated. Van de Hulst[11] classifies mist, fog and clouds as consisting of particles of water about 5 microns to 20 microns and rain from 200 microns to 2000 microns (2 mm). For rain conditions, much more liquid water is present and the attenuation characteristics are different than for the various hazy days described previously in terms of visible range. Since rain

drop size distribution is extremely difficult to measure, correlations for attentuation of radiation are based upon rain rate (mm/hr). It has been found theoretically and experimentally that attentuation of radiation by rain is independent of wavelength. Figure 10 shows 2 curves; one is the absorptive loss and the other is a combined absorptive plus scattering loss for all laser wavelengths considered between 0.3 micron and 11.0 micron as a function of rain rate. This plot has been extracted from work performed by Rensch and Long.[12]

For reference purposes a light rain is considered having a rain rate less than 40 mm/hr whereas a heavy rain has a rain rate of 90-100 mm/hr. To illustrate how rain effects rangefinder performance a heavy rain was considered (attenuation coefficient of 26 dB/Km or 2.51×10^{-3} 1/km) for a MLS day with high terrain background conditions for 1.06, 3.8 and 10.6 micron wavelengths. Table 6 shows how target range is effected by rain for the various wavelengths considered. Range for a heavy rain day is compared to range for a clear day having zero aerosol content. The overall conclusions from such a comparison are basically the same as those when considering visibility (due to aerosol content). A 10.6 micron wavelength rangefinder performs better in bad weather than does a 3.8 micron or 1.06 micron.

Table 6. Difference in Range for a MLS Day With "Heavy Rain" to an MLS Day Having Zero Aerosol Content.

$W_p/\sqrt{t_p}$ = 1000 J - $sec^{-1/2}$

λ (μm)	1.06	3.8	10.6
ΔR (km)	8.33	.375	.018

Receiver variables

Having determined that a rangefinder operating at 10.6 micron wavelength produces better performance for all weather and adverse battlefield conditions, receiver parameters were then investigated. The effects of specific detectivity (D^*), signal-to-noise ratio (S/N), field of view (FOV) and detector physical size (w) on target range was calculated. It should be noted that all the parameters mentioned were varied singularly in the study with the basepoint indicated by a circle on the respective curves. For these calculations, the following parameters were held constant:

$$W_p/\sqrt{t_p} = 1000 \text{ J - sec}^{-1/2}, \; V_R = 5 \text{ km, and } \lambda = 10.6 \text{ microns .}$$

Figure 11 shows the effect of varying D^* on range for both MLW and MLS days. Range varies moderately with D^*. For instance if D^* could be increased from 1×10^{10} cm-$Hz^{1/2}$-w^{-1} to 1×10^{11} cm-$Hz^{1/2}$-w^{-1}, range would increase from 3.7 km to 4.7 km for an MLS day and from 6.3 km to 9.4 km for an MLW day.*

Figure 12 shows how signal-to-noise ratio varies with range for both MLW and MLS days and also the required S/N for 99 percent detection probability. False signal indication of 1 percent for an assumed pulse width of 70 n-sec was used. With this criteria, the maximum range for an MLS and MLW day is 4.05 and 7.70 km respectively.

Figure 13 shows the effect of FOV on range for both MLW and MLS days. FOV is expressed in terms of the total conical angle θ as, FOV = $\pi \sin^2(\theta/2)$. As can be seen, range is very sensitive to FOV and will be a key parameter in optimizing the receiver design.

* It should be noted that the best "off the shelf" HgCdTe detector has a $D^* = 2 \times 10^{10}$ cm-$Hz^{1/2}$-w^{-1} and under special conditions $D^* = 5 \times 10^{10}$ cm-$Hz^{1/2}$-w^{-1}. Higher D^* will require advancing detector state-of-the-art.

The effect of detector physical size on range for both MLW and MLS days is shown in Figure 14. For this study both f/no. = 1.0 and D_R = 10.09 cm were kept constant. This produced changes in θ or FOV for changes in physical size W (square detector) which is then related to range. Range is seen to be very sensitive to detector size and this parameter will also be important when optimizing the receiver design. In all cases the detector sizes investigated were greater than the minimum size necessary to capture the third dark ring (93 percent of energy) of the Airy diffraction pattern. For the third dark ring, the minimum size detector is .0069 cm.

Conclusions

On the basis of the calculations performed, the following can be concluded with regard to rangefinder/designator performance.

1. When considering all weather operation (including rain) under real battelfield conditions (smoke, dust and hydrocarbons) a 10.6 micron wavelength is preferred for rangefinding and target designation.

2. The link analysis shows that for optimum performance, high W_p and short t_p are desirable. The recommended range of values for the pulsed laser correlation parameter, $W_p/\sqrt{t_p}$ is between 100 and 1000. Further tradeoffs with receiver variables is required before a specific value can be assigned.

3. The most striking result is the manner which range, R, varies with the laser pulse parameters, W_p and t_p. There is a logarithmic relationship between $W_p/\sqrt{t_p}$ and R. Thus, $W_p/\sqrt{t_p}$ can be reduced substantially while producing only small variations in range. Since t_p is a square-root function, it contributes an even smaller change in range. These trade-offs willl be very important in the light of weight and volume considerations.

4. Rangefinder performance improves when the specific detectivity is increased, field-of-view is decreased and absolute detector size is decreased. Range performance improves in terms of accuracy when signal-to-noise ratio is increased. The most sensitive of the above parameters are detector size and field-of-view.

Acknowledgments

The author wishes to thank Stan Scalise of the Optics and Applied Technology Laboratory for encouragement and many helpful discussions.

References

1. Palazzo, R. G., and Wasilko, R., Analysis of Laser Target Designation Systems at Various IR Wavelengths (U), DoD Conference, Colorado Springs, Colorado, March 1974. (Confidential)

2. Taylor, M. J., et. al., Pulsed CO_2 TEA Laser Rangefinder, Applied Optics, Vol. 17, No. 6, pp. 885 - 889, March 15, 1978.

3. Fradin, D. W., et. al., Middle Infrared Laser Target Designator Study (MIR-TLD) (U), R&D Tech. Report ECOM-0507-F, Final Report, Contract No. DAAB07-74-C-0507, United Aircraft Research Laboratories, June 13, 1974. (Confidential)

4. McClatchey, R. A., et. al., Optical Properties of Atmosphere (Third Edition), AFCRL-72-0497, Environmental Research Paper, No. 411, August 24, 2972.

5. Calculated Absorption Coefficients fo DF Laser Frequencies, Air Force Systems Command, RADC-TR-73-389, Technical Report, November 1973.

6. Wolfe, W. L. (Editor), Handbook of Military Infrared Technology, 255, Office of Naval Research, Department of the Navy, Washington, D.C., 1965.

7. Electro-Optics Handbook, RCA Solid State Division, Technical Series EOH-11, May 1978.

8. Holst, G. C., et al., Image and Laser Screening by Tactical Smoke (U), Proceedings of the Seventh DoD Conference on Laser Technology, Vol. 3, 8, 9, 10, June 1976. (Confidential)

9. Pepper, W. H., and Humphrey, R. G., Effect of Smoke on Ground Force Operations (U), Proceedings of the Sixteenth IRIS Symposium on Infrared Countermeasures (U), April 4-6, 1978. (Secret)

10. Shelton, Col. H. R., Recent Developments in Smoke Test Methodology, Proceedings of the Sixteenth IRIS Symposium on Infrared Countermeasures (U), April 4-6, 1978. (Secret)

11. Van de Hulst, H. C., Light Scattering by Small Particles, John Wiley and Sons, Inc., New York, 1957.

12. Rensch, D. B., and Long, R. K., Comparative Studies of Extinction and Backscattering by Aerosols, Fog and Rain at 10.6 Micron and 0.63 Micron, Applied Optics, Vol. 9, No. 7, July 1970.

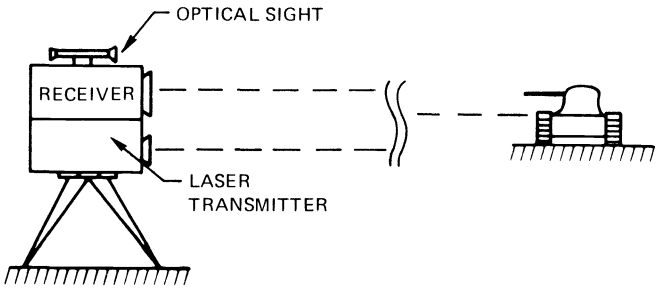

Figure 1a. Rangefinder configuration

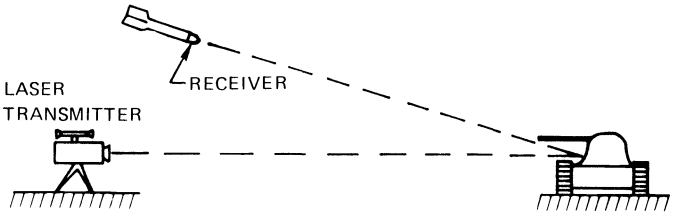

Figure 1b. Target designator configuration

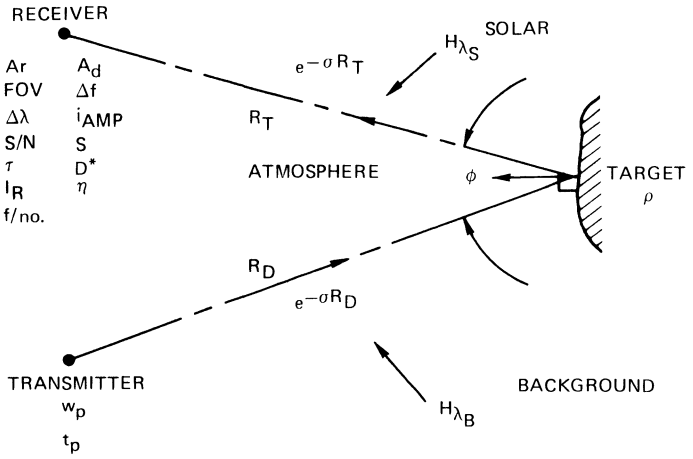

Figure 2. Schematic of link model

% REFLECTIVITY AT	1.06 μ	3.8 μ	10.6 μ
MAX	53	28	12
MEAN	34	15	6
MIN	11	4	2

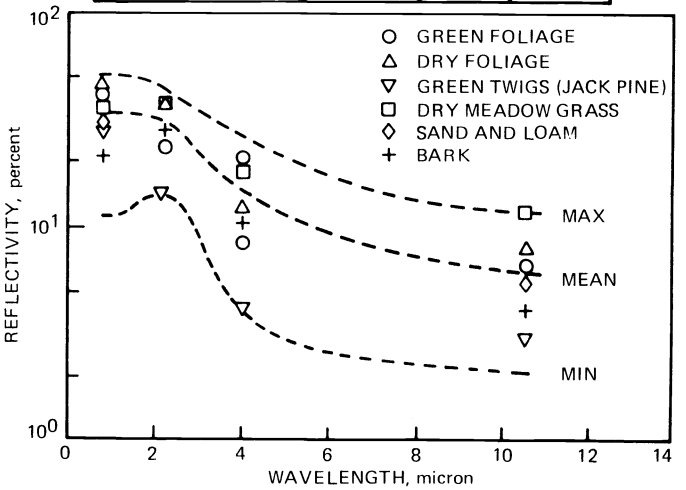

Figure 3. Broadband hemispherical reflectivity data

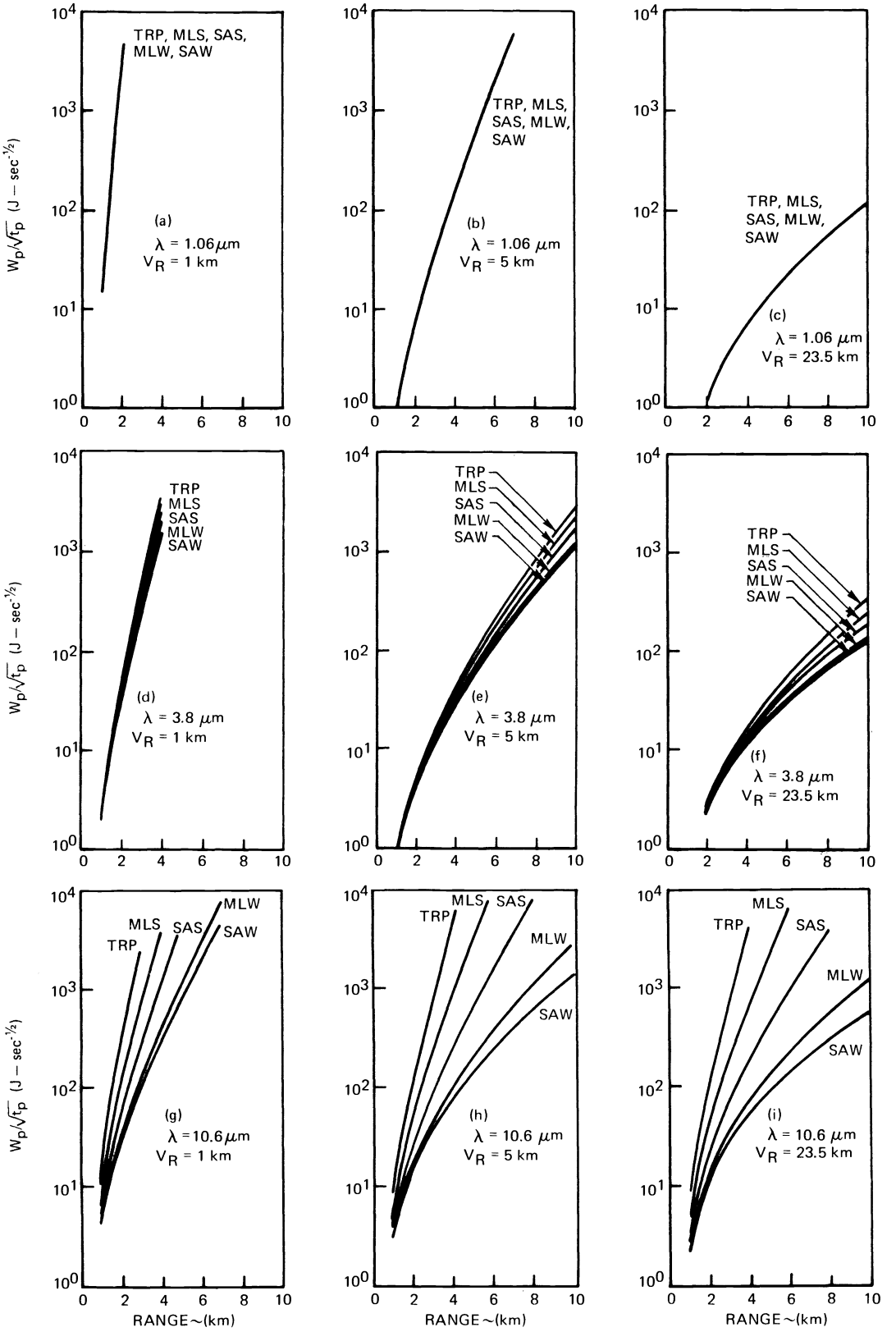

Figure 4. Rangefinder performance as a function of λ and V_R for high terrain background conditions

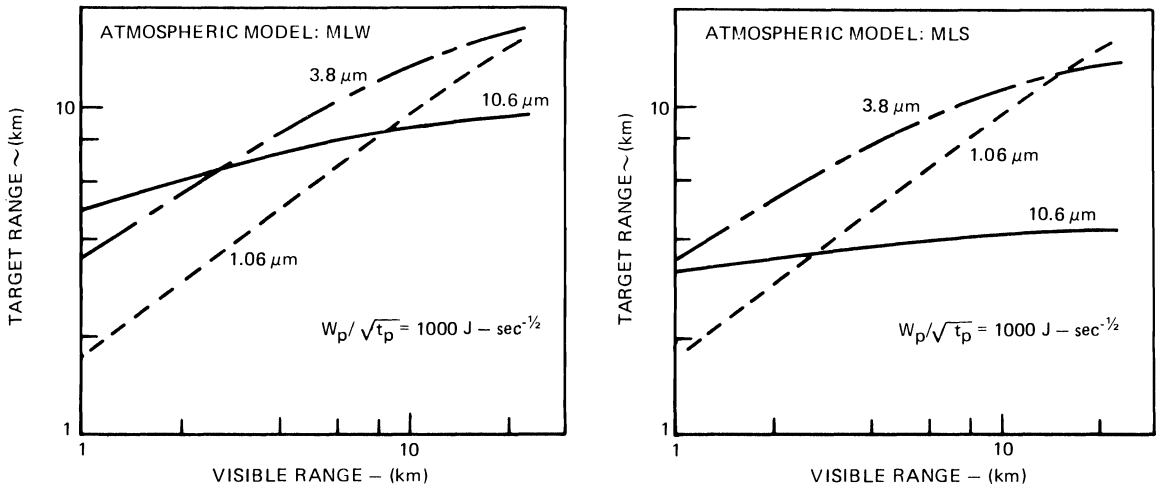

Figure 5. Target range versus visible range for 1.06, 3.8 and 10.6 micron rangefinder

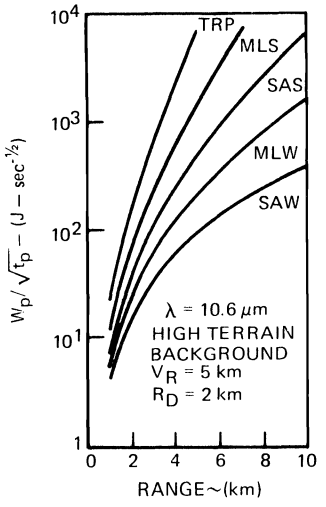

Figure 6. Target designator performance with weather conditions as a parameter

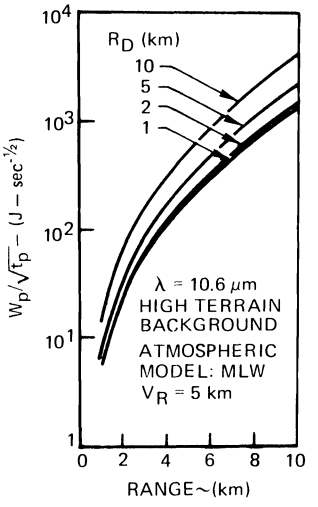

Figure 7. Target designator performance with designation range as a parameter

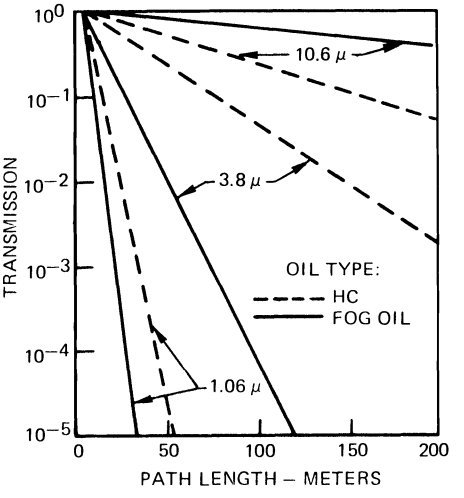

Figure 8. Transmission of laser radiation through tactical smokes

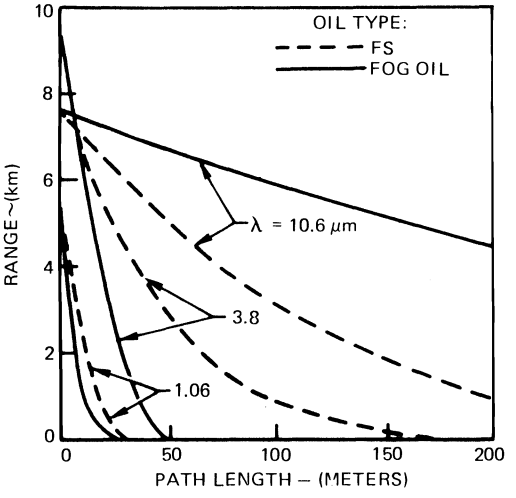

Figure 9. Reduction in ranging capability due to presence of smoke field obscuring target
Atmospheric model: MLW, Visibility: 5 km

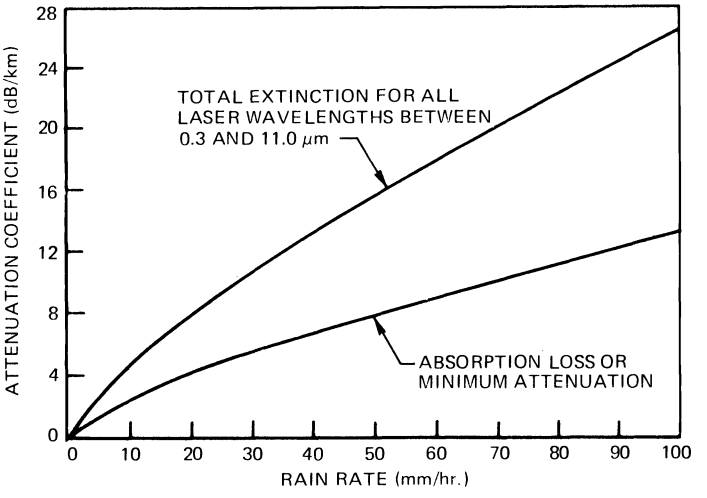

Figure 10. Attenuation coefficient for rain as a function of rain rate

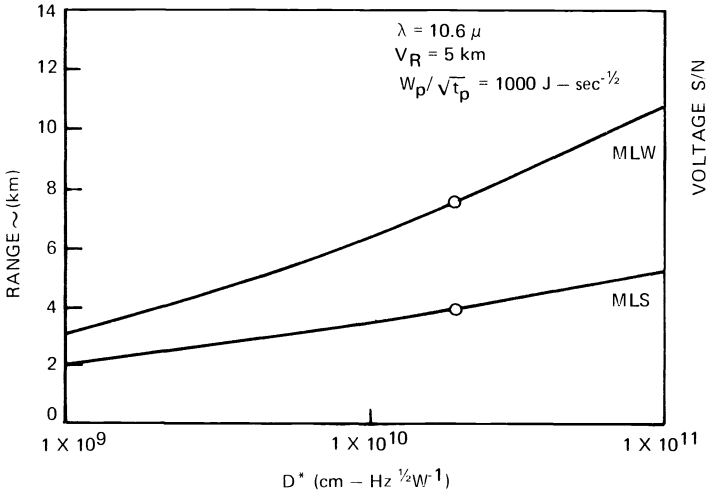

Figure 11. Effect of specific detectivity (D*) on range

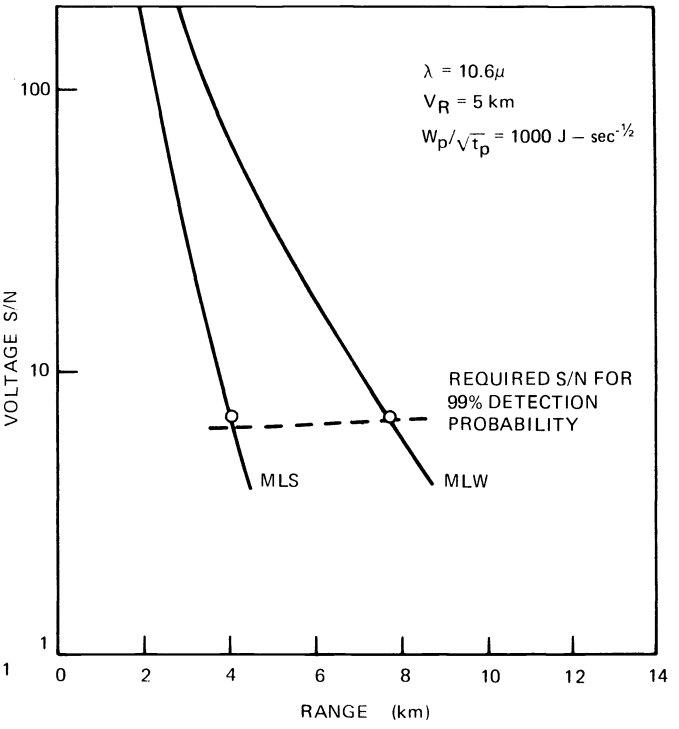

Figure 12. Effect of detector voltage S/N on range

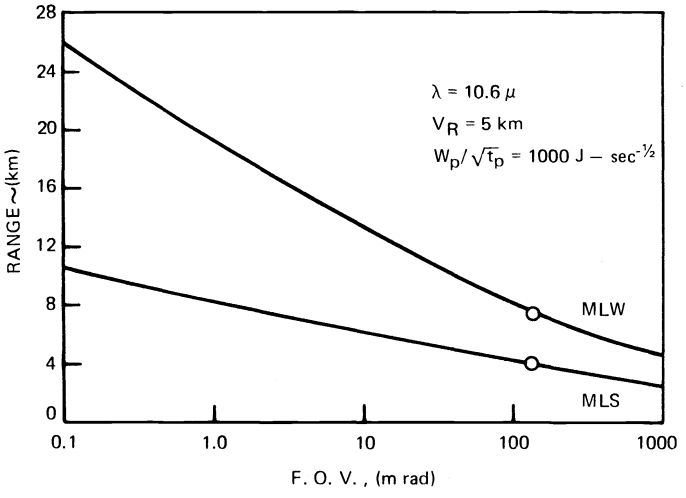

Figure 13. Effect of field–of–view on range

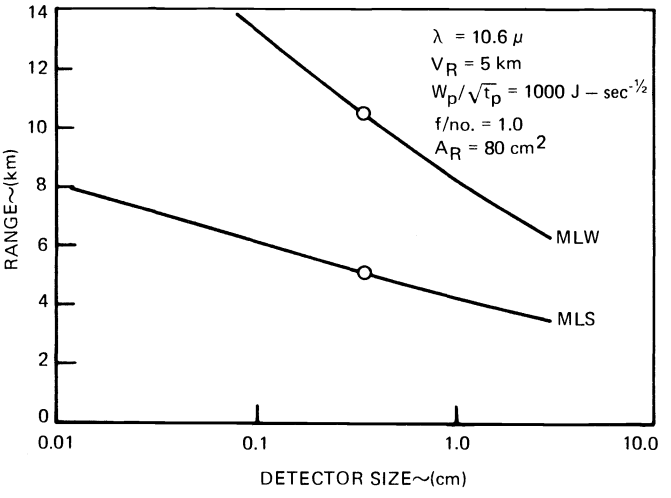

Figure 14. Effect of detector physical size on range